ELSEVIER

Journal of Nuclear Materials 283–287 (2000) 806–810

journal of nuclear materials

www.elsevier.nl/locate/jnucmat

A comparison of defects in helium implanted α- and β-SiC

P. Jung *, H. Klein, J. Chen

Institut für Festkörperforschung, Forschungszentrum Jülich (Association EURATOM–FzJ), D-52425 Jülich, Germany

Abstract

Specimens of α- and β-SiC were implanted homogeneously at room temperature with helium to about 30% of their thickness to concentrations up to 2450 atppm. Lattice straining was determined from the bending radius of the specimens by surface profilometry after implantation and during subsequent annealing. Evolution and annealing of straining in α- and β-SiC were remarkably similar. Above 1300°C specimen volume increased, which, according to transmission electron microscopy, was ascribed to the growth of helium clusters. Microstructural investigations showed bubbles along grain boundaries and disk-shaped clusters of bubbles in the grain interior on (0 0 0 1) habit planes in hexagonal α-SiC and on (1 1 1) in cubic β-SiC.

1. Introduction

Silicon-carbide based materials are considered for structural material in future fusion reactors due to their potential for high temperature application and low nuclear activation. A large number of polymorph phases of SiC exists, one of cubic (β-SiC) and a variety of hexagonal or rhombohedral (α-SiC) structures. For example, most hot pressing materials are α-SiC, while chemical vapor deposition (CVD) usually gives β-SiC. Thus composite SiC materials may contain a mixture of α- and β-phases. If these phases show for example different dimensional changes under irradiation, internal stresses and eventually disintegration of the material will result. Dimensional changes may occur under irradiation due to retention and clustering of defects. This may be stimulated by the presence of helium, which in nuclear environments is produced by nuclear transmutation. Furthermore, helium bubbles, especially along grain boundaries (GB), may also cause embrittlement by intergranular fracture, as frequently observed in metals. Previous investigations on helium in SiC were limited to either low-energy implantation or to helium production by neutrons in boron doped materials [1–3]. Thus helium was confined either to a near-surface region or to the vicinity of GBs where the boron segregates. In the present study, SiC was homogeneously implanted with He to about 100 μm depth, i.e., far beyond the grain size, and therefore results of dimensional changes as well as microstructure are considered to represent bulk behaviour.

2. Experimental details

Three different SiC materials were used in the present study. Hot-pressed α-SiC as described previously [4,5], β-SiC produced by CVD from Mitsui Engineering & Shipbuilding in the form of 5 in. disks of 400–500 μm thickness, and a SiC/C particulate composite [6]. In contrast to grains of several micrometers in α-SiC, grains sizes in the CVD β-SiC were below 1 μm. No grain growth was observed up to 2200°C, which was the highest temperatures before SiC reacted with the tungsten in the furnace. Therefore, the SiC/C composite from a previous study [6], which contained β-phase grains of several μm, was used for investigations of defects in the grain interior of β-SiC.

For strain measurement 2 mm wide ribbons were carefully polished to thicknesses of 200–426 μm and were fixed with Wood's metal to a copper heat sink and implanted in vacuum homogeneously to a depth of about 100 μm by α particles, the energy of which was varied from 15.7 MeV to 0 by using a degrader wheel as described previously [4]. The melting point of the

* Corresponding author. Tel.: +49-2461 614 036; fax: +49-2461 612 410.

E-mail address: p.jung@fz-juelich.de (P. Jung).

0022-3115/00/$ - see front matter
PII: S0022-3115(00)00211-7

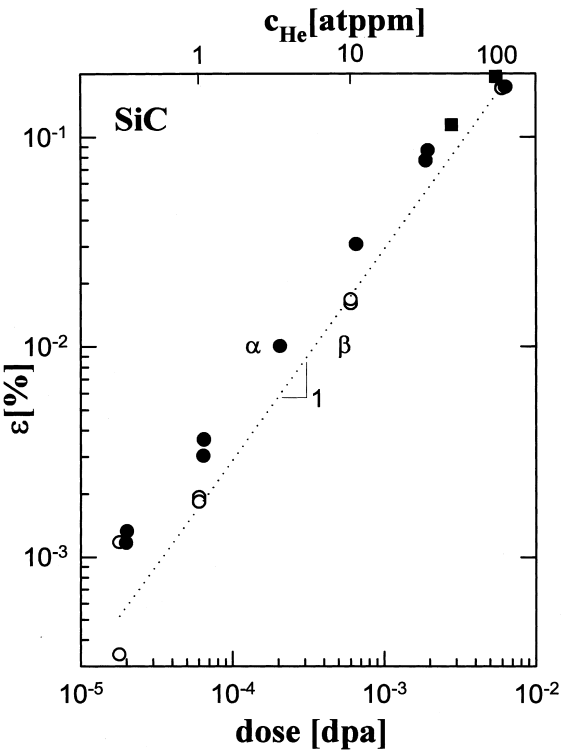

Fig. 1. Linear strain as a function of displacement dose in α- (●) and β-SiC (○), implanted with helium at $\leqslant$ 70°C. He concentrations are given on the upper scale. Included are results from α-SiC under permeating proton irradiation at ≈250°C (■) [9,10].

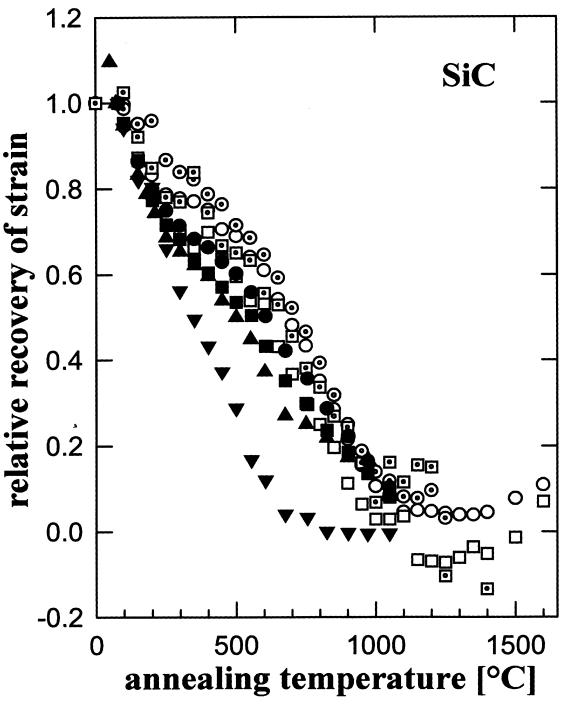

Fig. 2. Annealing of straining in β-SiC implanted with 10 (open and dotted circles), 100 (open and dotted squares) atppm He compared to α-SiC [4] with 1 (▼), 3 (▲), 10 (■) and 30 (●) atppm.

Wood's metal limited the temperature during implantation and subsequent unmounting to about 70°C. Calculations gave an average of about 60 displacements defects per α particle in the implanted region [7]. The specimens were annealed isochronally in a vacuum below 10^{-3} Pa with temperature steps of mostly 50°C and holding times of 0.5 h. Annealing temperatures was limited to ≈1600°C while at higher temperatures evap-

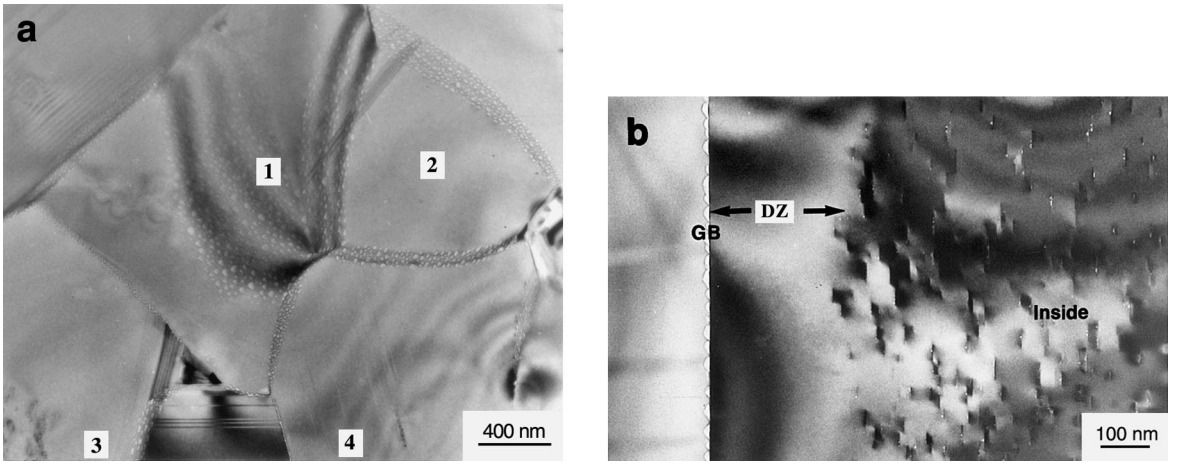

Fig. 3. Defects in α-SiC implanted to 600 atppm He and annealed for 1 h at 1350°C. In the middle of (a) a GB (1) is almost perpendicular to the beam, the small grain (2) is free of defects, while in the larger grains (3) and (4) defects are visible inside the grain at some distance from the GB. This defect free zone (DZ) along an edge-on GB is clearly seen in (b).

oration of furnace material (Al_2O_3 or W) to the specimen surfaces distorted the strain measurements. Bending of the specimens, implanted to about 30% of their thickness, was used to determine straining by surface profilometry (Dektak^{3}ST©, 5–10 mg load). The sensitivity of the present technique of strain measurement from bending of partially implanted ribbons (bimetal effect) is much higher than from uniaxial or step height measurements. At present limitation is set by the quality of surface preparation [7].

Specimens for transmission electron microscopy (TEM) were polished to about 150 μm before implantation, and annealed by dropping into a hot vacuum furnace (holding time 1 h). This gave very high heating and cooling rates [8]. After annealing TEM specimens were thinned by ion-milling.

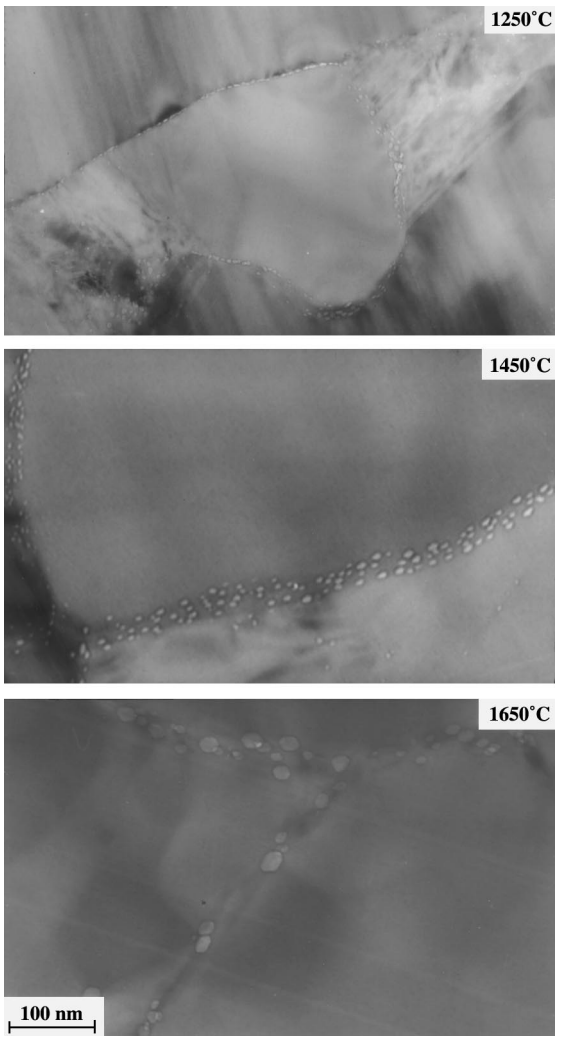

Fig. 4. Grain boundary bubbles in β-SiC, helium implanted to 600 atppm and annealed for 1 h at 1250, 1450 and 1650°C, respectively.

3. Results on helium-related defects

3.1. Lattice straining

Strain as a function of displacement dose for α- and β-SiC, calculated according to [7], are given in Fig. 1. Helium concentrations in the implanted region are given on the upper scale. The results for α-SiC were shown to be in good agreement with strains from proton and neutron irradiation when compared on the basis of displacements per atom (dpa) [4]. This indicates that straining in specimens implanted with helium near room temperature is essentially due to displacement defects, while the implanted He atoms have only a minor effect at these temperatures. In the strain calculations, only an average concentration of displacement defects in the homogeneously implanted region was considered, disregarding a decrease by about 30% from front to back side. Similar to strain evolution in Fig. 1, annealing of strain is very similar in α- and β-SiC as shown in Fig. 2. At concentrations in the 1 atppm range, recovery stages were observed mainly around 200°C, 530°C and 800°C. For α-SiC these stages were ascribed to the recombination of close pair defects and to free migration of carbon- and silicon-vacancies [4]. Already at concentrations of a few atppm, corresponding to $\geqslant 10^{-4}$ dpa, recovery becomes more gradually, presumably due to defect interaction and clustering. This is in agreement with the almost linear temperature dependence observed after

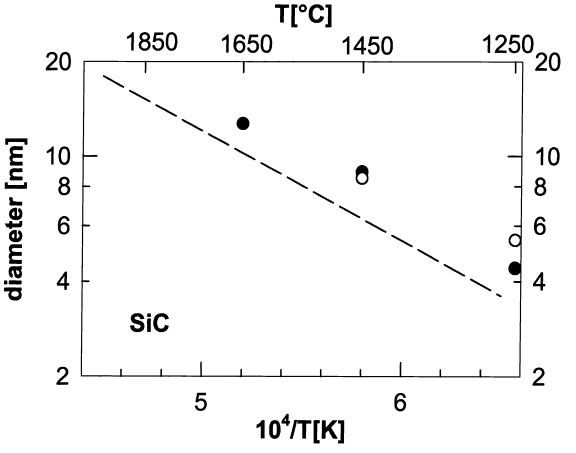

Fig. 5. Temperature dependence of average diameters of grain boundary bubbles in β-SiC implanted to 200 (○) and 600 (●) atppm He, respectively. The dashed line gives the diameters of the small bubble population inside grains of α-SiC (600 atppm, 1 h) [8].

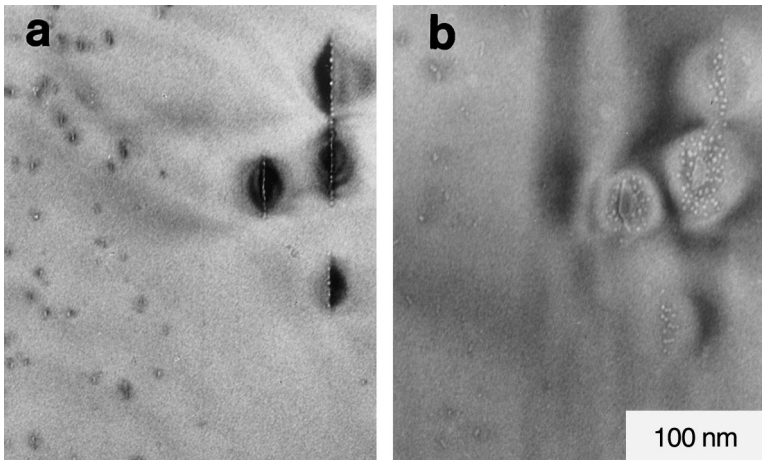

Fig. 6. Disks of helium bubbles in α-SiC (600 atppm He, 1 h 1250°C), shown edge on (a) and tilted by 30° (b). The large disks on the right-hand side have formed along dislocations.

neutron irradiation to much higher displacement doses [11–16]. Above 1300°C volume increase was observed which, according to TEM, was ascribed to bubble swelling by vacancy accumulation at helium clusters.

3.2. Defects in grain boundaries

In α-SiC implanted to above 2000 atppm He bubbles were observed in TEM [5,17], while at concentrations above 200 atppm, defects became visible only after annealing above 1250°C [8]. The grain interior was separated from the GB by defect free or depleted zones (DZ) as shown in Fig. 3. The width of DZs and also the size and morphology of bubbles along GB strongly depended on grain orientation, with bubble size increasing with inclination between boundary and (0 0 0 1) lattice planes [5,8]. No bubbles were found in twin boundaries of α-SiC [6].

In CVD β-SiC no defects were found in the grain interior. A possible explanation is that the width of the DZs presumable exceeds the small grain sizes of <1 μm. The GB bubbles in cubic β-SiC were close to circular with some faceting at larger sizes (Fig. 4). Fig. 5 shows bubble diameters in β-SiC specimens with 200 and 600 atppm He as a function of reciprocal annealing temperature (holding time ≈1 h). The sizes are slightly above those of the population of small bubbles inside α-SiC grains, but have the same temperature dependence (apparent activation energy ≈0.7 eV) [5,8]. From the dependence of bubble sizes in α-SiC on annealing temperature and time, the activation energy of the underlying growth process was estimated to about 4.4 eV. It was attributed to diffusion of lattice atoms along dislocation cores [8]. A slightly lower value might be expected in the present case for GB diffusion. Astonishingly, the analysis showed no dependence of bubble size in GBs on the size of the adjacent grains, while bubble density in GBs could not be analysed quantitatively.

3.3. Defects in grain interior

The consequence of the appearance of DZs was, that no defects were observed inside grains of diameters below about 1 μm. Results on bubble evolution as a function of helium concentration, annealing temperature and time in α-SiC are detailed in [8]. The predominant defects in α-SiC were two-dimensional

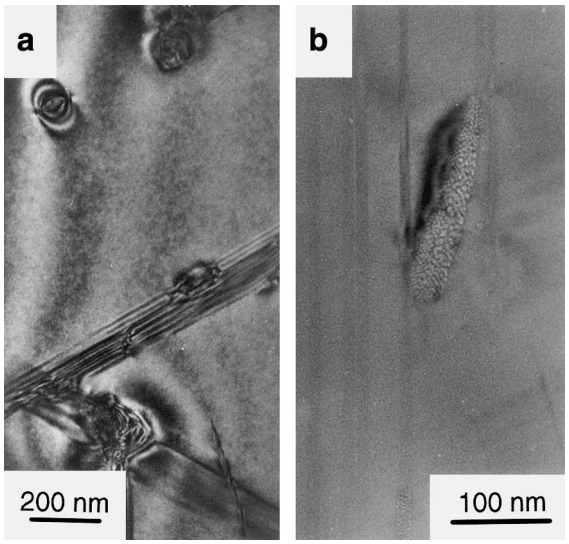

Fig. 7. Disks of helium bubbles inside β-SiC grains of SiC/C (1000 atppm He, 1 h 1050°C), forming along dislocations or stacking faults: (b) gives an enlarged view of one of the bubble disks in (a).

microcracks or platelets and above ≈1250°C disks of bubbles on (0 0 0 1) habit planes. At lower temperatures, such disks, sometimes of rather large size, are only observed associated to defects, preferentially along dislocations but not at stacking faults (Fig. 6). Also in the interior of β-SiC grains greater than 1 μm (in SiC/C), two-dimensional clusters of bubbles on (1 1 1) habit planes are observed. At temperatures up to 1050°C, these are always associated with dislocations or with dislocations at stacking faults (Fig. 7). Only at higher temperatures entangled arrangements of bubble disks on (1 1 1) planes are formed without pre-existing dislocations. Details are reported elsewhere [8].

4. Summary and conclusions

(1) Production and annealing of strain from helium implantation is similar in α- and β-SiC. Therefore no large internal stresses are to be expected in multiphase SiC composites.

(2) While helium bubbles on GB show a strong dependence of size and morphology on grain orientation in hexagonal α-SiC, no such dependence is observed in cubic β-SiC.

(3) In both materials, defects are only observed inside grains of above ≈1 μm, probably due to the existence of DZ along GB.

(4) The predominant defects observed inside grains are two-dimensional disks of bubbles on close packed direction, i.e., on habit planes (0 0 0 1) in α-, and (1 1 1) in β-SiC. At lower temperatures these bubble disks are in both phases only observed in association with dislocations.

References

[1] K. Hojou, S. Furuno, K.N. Kushita, H. Otsu, K. Izui, J. Nucl. Mater. 191–194 (1992) 583.
[2] J.C. Corelli, J. Hoole, J. Lazzaro, C.W. Lee, J. Am. Ceram. Soc. 66 (1983) 529.
[3] T. Suzuki, T. Yano, T. Mori, H. Miyazaki, T. Iseki, Fusion Technol. 27 (1995) 314.
[4] J. Chen, P. Jung, H. Klein, J. Nucl. Mater. 258–263 (1998) 1803.
[5] J. Chen, RWTH Aachen, PhD thesis, Report Forschungszentrum Jülich, Jül-3585, ISSN 0944-2952, 1998.
[6] J. Chen, P. Jung, in: P. Vincenzini (Ed.), Proceedings of the Nineth Cimtec-World Forum on New Materials, Advances in Science and Technology, Techna Series, vol. 24, 1999, p. 253, Ceram. Int. 26 (2000) 513.
[7] P. Jung, Z. Zhu, J. Chen, J. Nucl. Mater. 251 (1997) 276.
[8] J. Chen, P. Jung, H. Trinkaus, Phys. Rev. B 61 (2000-I) 12923.
[9] Z. Zhu, PhD thesis RWTH Aachen, Report Forschungszentrum Jülich, Jül-3109, ISSN 0944-2952, 1995.
[10] Z. Zhu, P. Jung, J. Nucl. Mater. 212–215 (1994) 1081.
[11] W. Primak, L.H. Fuchs, P.P. Day, Phys. Rev. 103 (1956) 1184.
[12] R.P. Thorne, V.C. Howard, B. Hope, Proc. Br. Ceram. Soc. 7 (1967) 449.
[13] R.J. Price, Nucl. Technol. 16 (1972) 536.
[14] H. Suzuki, T. Iseki, M. Ito, J. Nucl. Mater. 48 (1973) 247.
[15] T. Suzuki, T. Yano, T. Maruyama, T. Iseki, T. Mori, J. Nucl. Mater. 165 (1989) 247.
[16] H. Miyazaki, T. Suzuki, T. Yano, T. Iseki, J. Nucl. Sci. Technol. 29 (1992) 656.
[17] J. Chen, P. Jung, H. Trinkaus, Phys. Rev. Lett. 82 (1999) 2709.